

Corbino Disk Viscometer for 2D Quantum Electron Liquids

Andrea Tomadin,^{1,*} Giovanni Vignale,² and Marco Polini¹

¹*NEST, Istituto Nanoscienze-CNR and Scuola Normale Superiore, I-56126 Pisa, Italy*

²*Department of Physics and Astronomy, University of Missouri, Columbia, Missouri 65211, USA*

(Received 11 January 2014; revised manuscript received 14 April 2014; published 2 December 2014)

The shear viscosity of a variety of strongly interacting quantum fluids, ranging from ultracold atomic Fermi gases to quark-gluon plasmas, can be accurately measured. On the contrary, no experimental data exist, to the best of our knowledge, on the shear viscosity of two-dimensional quantum electron liquids hosted in a solid-state matrix. In this work we propose a Corbino disk device, which allows a determination of the viscosity of a quantum electron liquid from the dc potential difference that arises between the inner and the outer edge of the disk in response to an oscillating magnetic flux.

DOI: 10.1103/PhysRevLett.113.235901

PACS numbers: 66.20.-d, 47.80.-v, 71.10.-w, 73.23.-b

Introduction.—The shear viscosity η , which describes the diffusion of the average momentum density orthogonally to its direction, is one of the cornerstones of the hydrodynamic theory of fluids [1–3]. The first estimate of the shear viscosity of a dilute gas as a function of its density and temperature was given by Maxwell in his celebrated article on the “Dynamical Theory of Gases.” He found that the shear viscosity of a dilute gas is independent of its density, a counterintuitive result that he felt needed immediate experimental testing [4]. Recent years have witnessed a surge of interest in the viscous flow of strongly interacting quantum fluids, for which hydrodynamics provides a powerful nonperturbative description. Experimentally, the shear viscosity of quantum liquids like ³He and ⁴He can be measured by, e.g., capillary, rotation, and vibration viscometers [5]. The shear viscosity of cold atom gases can be inferred from measurements of collective modes or by looking at the expansion of the gas in a deformed trap after the trapping potential is turned off [6–8]. The shear viscosity of quark-gluon plasmas can be extracted from elliptic flow measurements at relativistic heavy-ion colliders [9]. To the best of our knowledge, however, no protocols exist for measuring the shear viscosity of two-dimensional (2D) quantum electron liquids (QELs) in solid-state matrices [10,11]. This gap is truly surprising in view of the large body of theoretical work [12,13] that has been carried out in connection with the shear viscosity of these systems. In this work we try and fill the gap by proposing a method to measure the viscosity of electrons in a realistic experimental setup.

The concept of hydrodynamic viscosity η [1–3] becomes relevant in a regime of parameters in which the 2DQEL is well described by a quasiequilibrium distribution function characterized by slowly space- and time-dependent density $n(\mathbf{r}, t)$ and drift velocity $\mathbf{v}(\mathbf{r}, t)$. In a solid-state device with linear dimension L this is ensured by the inequality $\ell_{ee} \ll L, \xi$. Here, ℓ_{ee} is the mean free path between quasiparticle collisions [14] and the length scale over which

local thermodynamic equilibrium is achieved. The quantity ξ is the correlation length of the smooth random potential V , inevitably present, [15] and the length scale over which momentum conservation is broken [15]. It is well known [15–17] that the above inequality can be satisfied in highly pure 2DQELs, e.g., in modulation-doped GaAs/AlGaAs semiconductor heterojunctions [10] for a suitable choice of electron densities and above liquid-helium temperature. Hydrodynamic electron flow has indeed been experimentally generated and hydrodynamic effects have been measured [18]. Deviations from the ideal hydrodynamic regime are parametrized in terms of an effective momentum relaxation rate $1/\tau$, which can be estimated (see Supplemental Material [19]) as $1/\tau = (\nu/\xi^2)(\Delta V/V)^2$, where ν is the kinematic viscosity (i.e., the viscosity η divided by the mass density) and $\Delta V/V$ is the magnitude of the potential fluctuations. The ideal hydrodynamic regime occurs for frequencies $\omega > 1/\tau$. For a correlation length ξ comparable to the size of the system, i.e., of the order of 10^{-6} m, with potential fluctuations $\Delta V/V \approx 10^{-2}$, and a kinematic viscosity of the order of 10^{-3} m²/s, we estimate $1/\tau \approx 0.1$ MHz, which leaves ample room to perform the measurements described in our Letter. We now describe our method for determining the viscosity.

Electrical measurement of the viscosity.—We consider a 2DQEL shaped in a Corbino disk (CD) geometry—see Fig. 1. The CD lies in the $z = 0$ plane and has an inner radius r_{in} and an outer radius r_{out} . It is separated from a back gate by a dielectric layer of thickness d and dielectric constant ϵ . An oscillating magnetic flux $\Phi(t) = \Phi_0 \cos(\Omega t)$ oriented along the \hat{z} axis threads the inner hole of the CD and induces, by Faraday’s law, an azimuthal electric field, which is given by [20]

$$\mathbf{E}_{\hat{\theta}}(r, t) = -\frac{1}{2\pi cr} \partial_t \Phi(t) \hat{\theta}, \quad (1)$$

where c is the speed of light and $\hat{\theta}$ is the unit vector in the azimuthal direction. Fluctuations of the circularly

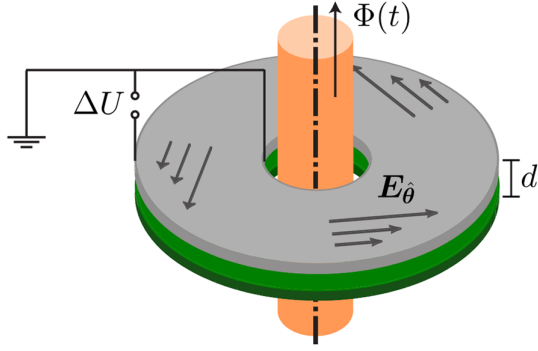


FIG. 1 (color online). A viscometer for 2D electron liquids. The light gray surface represents the 2D electron system, which is shaped into a Corbino disk geometry. The intermediate green region represents a dielectric layer of thickness d , which separates the 2D electron system from a back gate (dark gray region). The internal hole of the Corbino disk is threaded by an oscillating magnetic flux $\Phi(t) = \Phi_0 \cos(\Omega t)$, which induces an azimuthal electric field E_θ oscillating at the same frequency Ω . The magnitude of the azimuthal electric field decreases as one goes from the inner to the outer rim. The inner rim of the disk is grounded, while the outer rim is free to adjust its voltage. A dc electrical potential energy difference ΔU appears between the inner and the outer rim in response to the oscillating magnetic flux. The quantity ΔU sensitively depends on the shear viscosity of the 2D electron fluid and the frequency Ω of the magnetic flux.

symmetric electron density $n(r, t)$ on the surface of the CD generate a radial electric field of the form

$$\mathbf{E}_r(r, t) \approx \frac{e}{C} \partial_r n(r, t) \hat{r}, \quad (2)$$

where e is the absolute value of the electron charge, $C = \epsilon/(4\pi d)$ is the geometric capacitance per unit area, and \hat{r} is the unit vector in the radial direction. This “local capacitance approximation” is valid as long as d is much smaller than any lateral length scale [16]. The electron velocity $\mathbf{v}(r, t)$, with radial and azimuthal components $v_r(r, t)$ and $v_\theta(r, t)$, respectively, fluctuates in response to the total electric field $\mathbf{E}(r, t) = \mathbf{E}_\theta(r, t) + \mathbf{E}_r(r, t)$.

We now apply the Navier-Stokes equations of hydrodynamics [1,2] to the calculation of the time evolution of $n(r, t)$ and $\mathbf{v}(r, t)$. At first order in Φ_0 , the electron density fluctuations $n^{(1)}(r, t)$ and the radial velocity fluctuations $v_r^{(1)}(r, t)$ vanish, while the azimuthal velocity oscillates at the frequency of the magnetic flux, $v_\theta^{(1)}(r, t) = \text{Re}[v_\theta^{(1)}(r)e^{-i\Omega t}]$. At second order in Φ_0 , the circular motion of the electrons in the CD orbiting around the \hat{z} axis generates a dc potential energy difference ΔU between the inner and outer edges of the CD, given by

$$\Delta U = \frac{m}{2} \int_{r_{\text{in}}}^{r_{\text{out}}} dr \frac{1}{r} |v_\theta^{(1)}(r)|^2, \quad (3)$$

where m is the effective electron mass. The quantity ΔU in Eq. (3)—independent of time—can be readily recognized

as the work of the centripetal force acting on an electron which drifts from the inner to the outer rim of the CD and is subject to a constant acceleration in the radial direction given by $|v_\theta^{(1)}(r)|^2/(2r)$. For an ideal fluid ($\eta = 0$), it is easily shown (see discussion below) that the flow is given by

$$v_\theta^{(1)}(r)|_{\eta=0} = \frac{e}{mc} \frac{\Phi_0}{2\pi r} \equiv v_{\text{in}} \frac{r_{\text{in}}}{r}, \quad (4)$$

which is irrotational (i.e., curl-free) in the region $r_{\text{in}} < r < r_{\text{out}}$. Putting this in Eq. (3) and assuming $r_{\text{out}} \gg r_{\text{in}}$, we obtain

$$\Delta U|_{\eta=0} = \frac{e^2}{mc^2} \frac{1}{(2\pi r_{\text{in}})^2} \frac{1}{4} \Phi_0^2. \quad (5)$$

Notice that $\Delta U|_{\eta=0}$ is independent of the frequency Ω of the driving flux. To estimate the magnitude of the dc response, we use the following parameters [21]:

$$\begin{aligned} r_{\text{in}} &= 2.0 \mu\text{m}, & r_{\text{out}} &= 20.0 \mu\text{m}, \\ \Phi_0/(\pi r_{\text{in}}^2) &= 10 \text{ mT}, & m &= 0.067 m_e, \end{aligned} \quad (6)$$

where m_e is the bare electron mass in vacuum and the value of m given above is appropriate for electrons in GaAs [10]. From Eq. (5), we find $\Delta U|_{\eta=0} = 63 \mu\text{eV}$. The analytical result (4) is plotted as a solid line in Fig. 2.

Including the shear viscosity has three main effects on which we further elaborate below: (i) the spatial variation of the velocity field is considerably reduced (see Fig. 2), (ii) the flow acquires a non-curl-free dependence on the radial position r , i.e., a nonzero vorticity [1,2] $\boldsymbol{\omega} = \nabla_r \times \mathbf{v}$

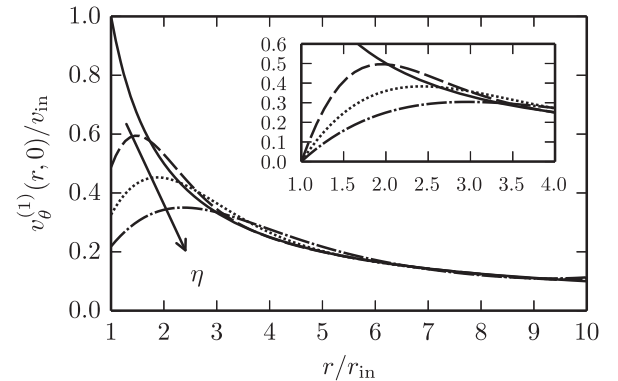


FIG. 2. Radial profile of the azimuthal component of the velocity—in units of v_{in} as defined in Eq. (4)—at $t = 0$, obtained by solving Eq. (15) with boundary conditions (12) (main panel) and (13) (inset). The results are obtained with $r_{\text{out}}/r_{\text{in}} = 10.0$, and for several values of the dimensionless parameter ζ defined in Eq. (16): $\zeta = 0.2$ (dashed line), 0.5 (dotted line), and 1.0 (dash-dotted line). The value of the viscosity in the different solutions increases as shown by the arrow. The solid line corresponds to the analytical result (4), which holds at $\zeta = 0$.

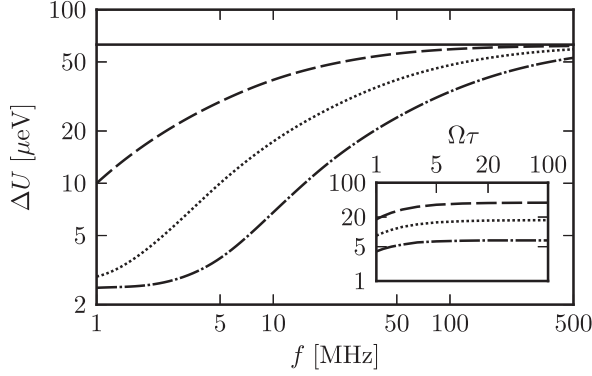


FIG. 3. The dc potential energy difference ΔU between the outer and inner rims of the Corbino disk as a function of the frequency $f = \Omega/(2\pi)$ of the oscillating magnetic flux $\Phi(t)$ (main panel) and the dimensionless variable $\Omega\tau$ (inset). Results in this plot have been obtained with the parameters as in Eq. (6). In the main panel $\Omega\tau = 10^3$. In the inset $f = 10$ MHz. Different curves correspond to different values of ν : 1.0 cm²/s (dashed line), 5.0 cm²/s (dotted line), and 15.0 cm²/s (dash-dotted line). The latter value corresponds to a simple order-of-magnitude estimate of the kinematic viscosity [16], i.e., $\nu \sim \hbar/m$. The solid line represents the viscous-free analytical result in Eq. (5).

appears near the inner and outer edges (see Fig. 4), and (iii) the dc potential drop ΔU becomes strongly frequency dependent (see Fig. 3). Indeed, ΔU decreases by a factor of 20 as the frequency decreases from 500 (where the effect of the viscosity is practically negligible) to 1 MHz. The profile of ΔU depends only on the ratio of the viscosity to the average mass density $m\bar{n}$, i.e., the kinematic viscosity [1,2]

$$\nu = \frac{\eta}{m\bar{n}}. \quad (7)$$

By measuring the frequency dependence of ΔU , subtracting the frequency-independent background (5), and fitting the theoretical curve to the experimental result one can determine ν . In the remainder of this Letter we supply the main steps of the calculation of ΔU .

Hydrodynamic equations and their solution.—In the hydrodynamic regime, the response of the 2DQEL is governed by the Navier-Stokes equation [1,2]

$$\begin{aligned} \rho(r, t) \{ \partial_t \mathbf{v}(r, t) + [\mathbf{v}(r, t) \cdot \nabla_r] \mathbf{v}(r, t) \} \\ = -e\mathbf{E}(r, t)n(r, t) - \nabla_r P(r, t) + \eta \nabla_r^2 \mathbf{v}(r, t), \end{aligned} \quad (8)$$

combined with the continuity equation

$$\partial_t n(r, t) + \nabla_r \cdot [n(r, t)\mathbf{v}(r, t)] = 0. \quad (9)$$

Here, $\rho(r, t) = mn(r, t)$ is the mass density and $P(r, t)$ is the pressure. In Eq. (8) we have neglected a term due to the bulk viscosity since it vanishes at long wavelengths [1,14]. Weak momentum nonconservation can be taken into account in a phenomenological manner by adding

[16,22] a friction term of the form $-\rho(r, t)\mathbf{v}(r, t)/\tau$ to the right-hand side of Eq. (8). In Ref. [19] we use hydrodynamic arguments [15] to demonstrate that $\tau \gtrsim 1 \mu\text{s}$ in the region of parameter space of interest. The quantity τ should not be confused with the much shorter time scale τ_D that determines the usual Drude mobility $\mu = e\tau_D/m$ in the diffusive regime. The inset in Fig. 3 shows results obtained for finite values of τ .

In Eq. (8) we have also included the contribution of the electric field $\mathbf{E}(r, t)$. The azimuthal symmetry of the system implies that all quantities depend on the radial coordinate r only and that the derivatives with respect to the azimuthal angle θ vanish. The radial component $E_r(r, t)$ of the electric field is given by $E_r(r, t) = -\hat{r}\partial_r U(r, t)/e$, where the electric potential energy $U(r, t)$ is obtained by solving the Poisson equation in the CD geometry with a constant boundary condition at the gate position $z = -d$. If the typical wavelength of density fluctuations is larger than d , it is easy to see that

$$U(r, t) \simeq -e^2 n(r, t)/C, \quad (10)$$

which immediately leads to Eq. (2). Finally, the pressure gradient in Eq. (8) can be neglected when $\partial P(n)/\partial n \ll e^2 \bar{n}/C$, i.e., when $d \gg a_B^*/4$. This inequality is always well satisfied since $a_B^* \equiv \epsilon \hbar^2 / (me^2)$ is the material Bohr radius, which is ~ 10 nm for GaAs.

The Navier-Stokes and continuity equations (8)–(9) must be complemented by suitable boundary conditions (BCs) expressed in terms of the momentum flux density tensor [1,2] $\Pi_{i,k}(r, t) = P(r, t)\delta_{i,k} + \rho v_i(r, t)v_k(r, t) - \sigma'_{i,k}(r, t)$, where $\sigma'_{i,k}(r, t)$ is the viscous stress tensor. We require the radial diffusion of azimuthal momentum, which is proportional to the viscosity η , to vanish at the outer and inner rims of the CD, i.e.,

$$\sigma'_{r,\theta}(r, t)|_{r=r_{\text{in}}} = \sigma'_{r,\theta}(r, t)|_{r=r_{\text{out}}} \equiv 0. \quad (11)$$

The off-diagonal component of the viscous stress tensor reads $\sigma'_{r,\theta} = \eta(\partial_r v_\theta + \partial_\theta v_r/r - v_\theta/r)$ [1,2]. Because of circular symmetry, the BCs (11) reduce to

$$\partial_r v_\theta(r, t)|_{r=r_i} = \frac{v_\theta(r, t)}{r} \Big|_{r=r_i}, \quad (12)$$

where $r_i = r_{\text{in}}, r_{\text{out}}$. Moreover, for the setup in Fig. 1, two further BCs should be imposed. First, the radial component of the current $\mathbf{j}(r, t) = n(r, t)\mathbf{v}(r, t)$ must vanish at the outer rim, where the CD is isolated. This, together with Eq. (11), implies that the sum of the forces acting on the fluid element vanishes at the outer rim. The sum of the forces, however, does not vanish at the inner rim, since here a contact connects the device to ground. This implies [22,23] that at this contact the electron density $n(r_{\text{in}}, t)$

must be equal to the average value $\bar{n} = eV_G/C$ fixed by the gate voltage V_G .

We notice that the BCs (12) differ from the standard “no-slip” BCs

$$v_\theta(r, t)|_{r=r_{\text{in}}} = v_\theta(r, t)|_{r=r_{\text{out}}} \equiv 0, \quad (13)$$

which are commonly employed [1,2] to describe fluid adhesion to the walls of a container. While the use of the BCs in Eq. (13) is not immediately justified in our case, we have checked that the results in Fig. 3 do not change qualitatively if the BCs in Eq. (13) are used instead of those in Eq. (12). The agreement between the results obtained with two different sets of BCs gives us confidence in the robustness of the effect illustrated in Fig. 3.

We solve Eqs. (8)–(9) by expanding the hydrodynamic variables in powers of the amplitude Φ_0 of the magnetic flux [22]:

$$\begin{aligned} \mathbf{v}(r, t) &= \mathbf{v}^{(0)}(r, t) + \mathbf{v}^{(1)}(r, t) + [\delta\mathbf{v}(r) + \mathbf{v}^{(2)}(r, t)] + \dots, \\ n(r, t) &= n^{(0)}(r, t) + n^{(1)}(r, t) + [\delta n(r) + n^{(2)}(r, t)] + \dots, \end{aligned} \quad (14)$$

where $\mathbf{v}^{(k)}(r, t), n^{(k)}(r, t) \sim (\Phi_0)^k \cos(k\Omega t)$. Since the hydrodynamic equations of motion are nonlinear, in the expansion (14) we include constant contributions $\delta\mathbf{v}(r), \delta n(r) \sim \mathcal{O}(\Phi_0^2)$ arising from the self-mixing of the signal at frequency Ω [22]. At first order, we find the following differential equation for the radial profile of the azimuthal component of the velocity:

$$\begin{aligned} -i\Omega v_\theta^{(1)}(r) &= \nu \left[\partial_r^2 v_\theta^{(1)}(r) + \frac{1}{r} \partial_r v_\theta^{(1)}(r) - \frac{1}{r^2} v_\theta^{(1)}(r) \right] \\ &\quad - i\Omega \frac{e}{mc} \frac{\Phi_0}{2\pi r}. \end{aligned} \quad (15)$$

In the general $\nu \neq 0$ case, Eq. (15) can be easily solved numerically. It is convenient to introduce dimensionless variables by rescaling r with r_{in} and $v_\theta^{(1)}(r)$ with v_{in} , which has been defined in Eq. (4). Then, Eq. (15) depends only on the dimensionless parameter

$$\zeta \equiv \left(\frac{L_\eta}{r_{\text{in}}} \right)^2, \quad (16)$$

where $L_\eta = \sqrt{\nu/\Omega}$ is the vorticity penetration depth [1,2] during a time $1/\Omega$. The solution of Eq. (15) is shown in Fig. 2 for several values of ζ and both sets of BCs. We note that with increasing viscosity the amplitude of the velocity flow diminishes. Since according to Eq. (3) ΔU depends on the integral of the square of the velocity profile, increasing the viscosity suppresses the dc response ΔU , thereby explaining the results in Fig. 3.

In the limit $\zeta \ll 1$ (low viscosity or high frequency) the solution of Eq. (15) is given by the curl-free profile in Eq. (4). In the opposite $\zeta \gg 1$ limit (high viscosity or low frequency) the solution is found by setting to zero the term in square brackets in Eq. (15). In this case, it is easy to demonstrate that a non-curl-free linear profile $v_\theta^{(1)}(r) \propto r$ solves the problem, satisfying the BCs.

To obtain the dc response ΔU in Eq. (3) we expand Eq. (9) and the radial component of Eq. (8) to second order and we average the resulting expressions over a period $T = 2\pi/\Omega$ of the oscillating flux $\Phi(t)$. The solution of the time-averaged equations yields $\delta v_r(r) \equiv 0$ and

$$\delta n(r) = \frac{mC}{e^2} \int_{r_{\text{in}}}^r dr' \frac{1}{r'} \langle v_\theta^{(1)}(r, t)^2 \rangle_t, \quad (17)$$

where $\langle g(t) \rangle_t \equiv T^{-1} \int_0^T dt' g(t')$ denotes the time average of a function $g(t)$ over one period of the oscillating magnetic flux. Finally, Eq. (3) can be easily obtained by setting $r = r_{\text{out}}$ in Eq. (17) and making use of $\langle v_\theta^{(1)}(r, t)^2 \rangle_t = |v_\theta^{(1)}(r)|^2/2$ and of the local capacitance formula Eq. (10).

Vorticity.—Further insights on the physical properties of the solution shown in Fig. 2 can be obtained by looking at the radial profile of the vorticity $\omega_z(r, t) = \partial_r[r v_\theta(r, t)]/r$, whose first-order contribution $\omega_z^{(1)}(r, t)$ in powers of Φ_0 is shown in Fig. 4. In the regions near the rims of the CD the non-curl-free dependence of the velocity flow $v_\theta^{(1)}(r, t)$ on r leads to large values of the vorticity. Moving away from the rims, the vorticity decreases to zero on a length scale L_η , which confirms the interpretation of this quantity as the vorticity penetration depth [1,2,24]. On the same length scale the velocity flow crosses over to the curl-free profile (4)—see inset in Fig. 4. Reference [19] reports a calculation of the dissipation due to viscosity and proposes an

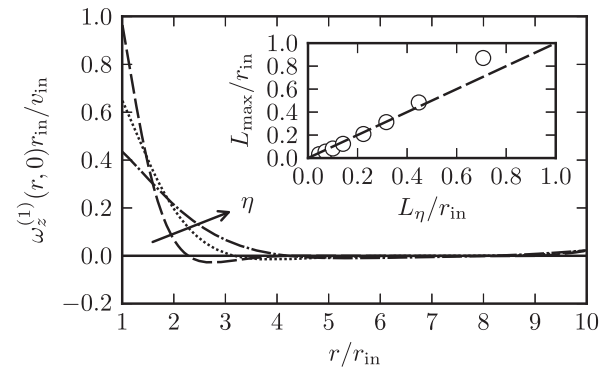


FIG. 4. Same as in Fig. 2 but for the radial profile of the vorticity $\omega_z^{(1)}(r, t)$ (in units of $v_{\text{in}}/r_{\text{in}}$) at time $t = 0$. The inset shows the position L_{max} of the maximum of $v_\theta^{(1)}(r, t = 0)$, as displayed in Fig. 2, for several values of the vorticity penetration depth L_η (in units of r_{in}). The dashed line corresponds to the expected relation $L_{\text{max}} = L_\eta$.

alternative method, with respect to the one discussed after Eq. (7), to measure η .

In summary, we have demonstrated that the shear viscosity of a two-dimensional quantum electron liquid can be obtained by studying the response of the system to an oscillating magnetic flux in a Corbino disk geometry. We truly hope that this work will stimulate further studies of viscometers for two-dimensional quantum electron liquids and related experimental activities on the shear viscosity of these systems, which may pave the way for the discovery of solid-state nearly perfect fluids [5].

G. V. was supported by the NSF through Grant No. DMR-1104788. We gratefully acknowledge A. Hamilton for very useful discussions. We have made use of free software [25].

* andrea.tomadin@sns.it

- [1] L. D. Landau and E. M. Lifshitz, *Course of Theoretical Physics: Fluid Mechanics* (Pergamon, New York, 1987).
- [2] G. K. Batchelor, *An Introduction to Fluid Dynamics* (Cambridge University Press, Cambridge, England, 1967).
- [3] A. A. Abrikosov and I. M. Khalatnikov, *Rep. Prog. Phys.* **22**, 329 (1959).
- [4] J. C. Maxwell, *Philos. Trans. R. Soc. London* **156**, 249 (1866).
- [5] T. Schäfer and D. Teaney, *Rep. Prog. Phys.* **72**, 126001 (2009).
- [6] C. Cao, E. Elliott, J. Joseph, H. Wu, J. Petricka, T. Schäfer, and J. E. Thomas, *Science* **331**, 58 (2011).
- [7] C. Cao, E. Elliott, H. Wu, and J. E. Thomas, *New J. Phys.* **13**, 075007 (2011).
- [8] E. Vogt, M. Feld, B. Fröhlich, D. Pertot, M. Koschorreck, and M. Köhl, *Phys. Rev. Lett.* **108**, 070404 (2012).
- [9] R. Snellings, *New J. Phys.* **13**, 055008 (2011); B. V. Jacak and B. Müller, *Science* **337**, 310 (2012).
- [10] L. N. Pfeiffer and K. W. West, *Physica (Amsterdam)* **20E**, 57 (2003); V. Umansky, M. Heiblum, Y. Levinson, J. Smet, J. Nübler, and M. Dolev, *J. Cryst. Growth* **311**, 1658 (2009).
- [11] For 2DQELs other than 2D electron gases in semiconductor heterostructures, see, for example, K. S. Novoselov, D. Jiang, F. Schedin, T. J. Booth, V. V. Khotkevich, S. V. Morozov, and A. K. Geim, *Proc. Natl. Acad. Sci. U.S.A.* **102**, 10 451 (2005); A. K. Geim and K. S. Novoselov, *Nat. Mater.* **6**, 183 (2007); M. Z. Hasan and C. L. Kane, *Rev. Mod. Phys.* **82**, 3045 (2010); X.-L. Qi and S.-C. Zhang, *ibid.* **83**, 1057 (2011); J. Mannhart, D. H. A. Blank, H. Y. Hwang, A. J. Millis, and J.-M. Triscone, *MRS Bull.* **33**, 1027 (2008); J. Mannhart and D. G. Schlom, *Science* **327**, 1607 (2010), and references therein.
- [12] S. Conti and G. Vignale, *Phys. Rev. B* **60**, 7966 (1999); I. V. Tokatly and G. Vignale, *ibid.* **76**, 161305(R) (2007); **79**, 199903(E) (2009); F. D. M. Haldane, arXiv:0906.1854; N. Read, *Phys. Rev. B* **79**, 045308 (2009); M. Müller, J. Schmalian, and L. Fritz, *Phys. Rev. Lett.* **103**, 025301 (2009); T. L. Hughes, R. G. Leigh, and E. Fradkin, *ibid.* **107**, 075502 (2011).
- [13] B. Bradlyn, M. Goldstein, and N. Read, *Phys. Rev. B* **86**, 245309 (2012); C. Hoyos and D. T. Son, *Phys. Rev. Lett.* **108**, 066805 (2012).
- [14] G. F. Giuliani and G. Vignale, *Quantum Theory of the Electron Liquid* (Cambridge University Press, Cambridge, England, 2005).
- [15] A. V. Andreev, S. A. Kivelson, and B. Spivak, *Phys. Rev. Lett.* **106**, 256804 (2011).
- [16] M. Dyakonov and M. Shur, *Phys. Rev. Lett.* **71**, 2465 (1993).
- [17] A. O. Govorov and J. J. Heremans, *Phys. Rev. Lett.* **92**, 26803 (2004).
- [18] See, for example, M. J. M. de Jong and L. W. Molenkamp, *Phys. Rev. B* **51**, 13389 (1995); D. Taubert, G. J. Schinner, H. P. Tranitz, W. Wegscheider, C. Tomaras, S. Kehrein, and S. Ludwig, *ibid.* **82**, 161416 (2010); D. Taubert, G. J. Schinner, C. Tomaras, H. P. Tranitz, W. Wegscheider, and S. Ludwig, *J. Appl. Phys.* **109**, 102412 (2011).
- [19] See Supplemental Material at <http://link.aps.org/supplemental/10.1103/PhysRevLett.113.235901> for a calculation of the hydrodynamic relaxation time τ , estimates of the effects of external magnetic fields and self-inductance, and a discussion of the instantaneous power dissipated in the fluid.
- [20] The role of the self-inductance of the currents in the disk and the spill out of the flux threading the inner hole of the CD are discussed in Ref. [19].
- [21] The value of Φ_0 given in Eq. (6) corresponds $\Phi_0 \approx 60\phi_0$, where $\phi_0 = h/(2e) \approx 2 \times 10^{-15}$ Wb is the magnetic flux quantum.
- [22] M. Dyakonov and M. Shur, *IEEE Trans. Electron Devices* **43**, 380 (1996).
- [23] A. Tomadin and M. Polini, *Phys. Rev. B* **88**, 205426 (2013).
- [24] This can be seen as follows: $\omega_z^{(1)}(r, t)$ obeys the 2D equation of motion [2] $\partial_t \omega_z^{(1)}(r, t) = \nu \nabla_r^2 \omega_z^{(1)}(r, t)$. Therefore, ν plays the role of diffusion constant for $\omega_z^{(1)}(r, t)$. This happens because the 2D flow in our case is uniform and incompressible to $\mathcal{O}(\Phi_0)$.
- [25] www.gnu.org, www.python.org.